

Stop-hole conditions to prevent re-initiation of fatigue cracks

Ichiro Okura[†] and Toshiyuki Ishikawa[‡]

Osaka University, Department of Civil Engineering, 2-1 Yamadaoka, Suita, Osaka 565-0871, Japan
(Received September 11, 2001, Revised October 28, 2002, Accepted November 18, 2002)

Abstract. In steel bridges fatigue cracks are sometimes repaired by placing drilled holes at the crack tips. From the meaning that the drilled holes stop the propagation of cracks, they are called stop-holes. Since stop-holes are regarded as an emergency measure to delay crack propagation, usually some substantial repair follows. However, if the stress at the stop-holes is below their fatigue limit, fatigue cracks would not be expected to occur. The purpose of this study is to present the conditions under which stop-holes prevent the re-initiation of fatigue cracks. The fatigue limit of stop-holes and the equations necessary to estimate the maximum stress on the circumference of the stop-holes are provided.

Key words: fatigue; stop-hole; crack; stress concentration.

1. Introduction

To repair the fatigue cracks initiated in steel bridges, drilled holes are sometimes placed at the crack tips. The drilled holes stop the propagation of cracks by easing the stress concentration at the crack tips. From the meaning that drilled holes stop the crack propagation, they are called stop-holes.

In the USA, Fisher (1984) reported many instances in which fatigue cracks were repaired by stop-holes. He proposed the following equation to predict when stop-holes would prevent the re-initiation of fatigue cracks (Fisher, Barthelemy, Mertz and Edinger 1980).

$$\frac{\Delta\sigma_{mn}\sqrt{\pi a}}{\sqrt{\rho}} < 10.5\sqrt{\sigma_Y} \quad (1)$$

Referring to Fig. 1, $\Delta\sigma_{mn}$ is the range of membrane stress calculated by the theory of structures (MPa), a is the half of the length between the edges of two stop holes (m), ρ is the radius of the holes (m), and σ_Y is the yield stress of steel (MPa).

Later, however, he pointed out that when plate-bending stresses due to out-of-plane deformation of main girder webs are produced around stop-holes, fatigue cracks may be re-initiated at the holes, even though the holes satisfy the relationship of Eq. (1) (Fisher, Jin, Wagner and Yen 1990).

In Japan stop-holes are regarded as an emergency measure to temporarily delay the propagation

[†]Associate Professor

[‡]Graduate Student

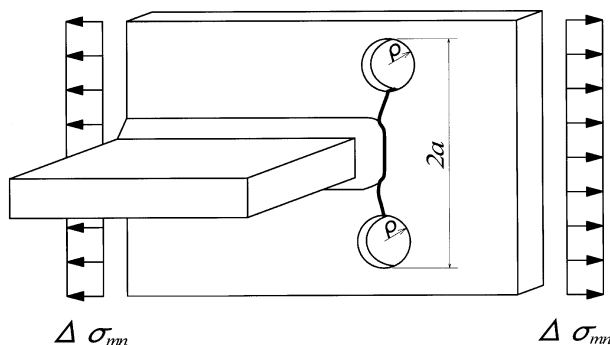


Fig. 1 Stop-holes

of fatigue cracks, and some substantial repair is required later (Japan Road Association 1997). There is a case in which high-strength bolts are put in stop-holes to extend the fatigue life of the holes.

Whether cracks are re-initiated at stop-holes or not will depend on the stress conditions at the holes. If the stress on the circumference of stop-holes is below their fatigue limit, fatigue cracks will not likely occur.

The purpose of this study is to present the conditions under which stop-holes prevent the re-initiation of fatigue cracks. The fatigue limit of stop-holes and the equations necessary to estimate the maximum stress on the circumference of the stop-holes are provided.

2. Fatigue strength of a circular hole

2.1. Fatigue tests of plates with a circular hole

Fig. 2 shows fatigue test specimens (Okura, Shiozaki and Nakanishi 1996, Okura and Ishikawa 1999). Specimens T40 and T49 were employed for tensile fatigue tests, while Specimens B40 were used for bending fatigue tests. The drilled hole in the middle of the specimens is the object of the test. In Specimens T40 and B40, the corner of the hole edge were chamfered by the drill with a diameter somewhat larger than 24.7 mm. The chamfering was not done for Specimens T49. First the surface of the plate thickness of the hole was polished along the circumference with a #100 sandpaper and finally finished with a #1000 sandpaper (Japanese Industrial Standard 1994). Table 1 lists the material properties of the specimens. The steels used were Japanese SS400 for Specimens T40 and B40, and SM490Y for Specimens T49. The former has a guaranteed yield stress of 235.4 MPa and a guaranteed tensile strength of 400 MPa. The latter has a guaranteed yield value of 353.0 MPa and a guaranteed tensile strength of 490 MPa.

Fig. 3 presents an overall view of the fatigue tests. In the tensile fatigue test, hinges were installed at the top and bottom ends of the specimens so that plate-bending stresses would not be induced in the specimens. In the four point bending fatigue test, a constant bending moment was created over a length of 300 mm between the two support points. The fatigue tests were carried out under load control with servo-type fatigue testing machines.

The results of the fatigue tests are given in Table 2. Here the meaning of the symbols is as follows: R

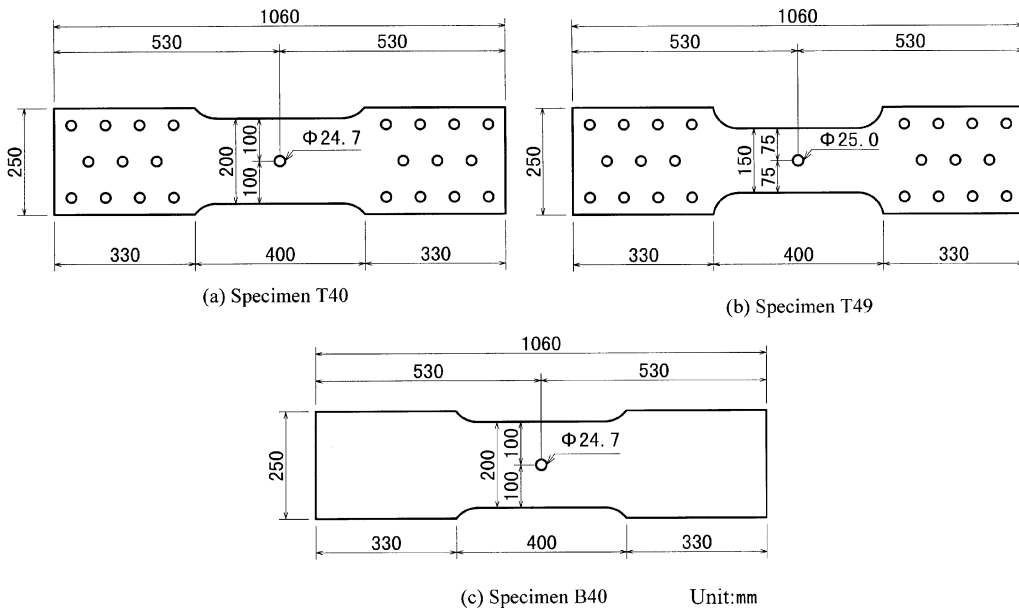


Fig. 2 Fatigue test specimens

Table 1 Material properties of specimens

Specimen	Steel	Young's modulus ($\times 10^5$ MPa)	Yield stress (MPa)	Tensile strength (MPa)	Elongation (%)
T40	SS400	2.005	273.7	415.7	29.7
T49	SM490Y	2.104	402.4	529.2	20.2
B40	SS400	2.027	274.8	423.4	29.8

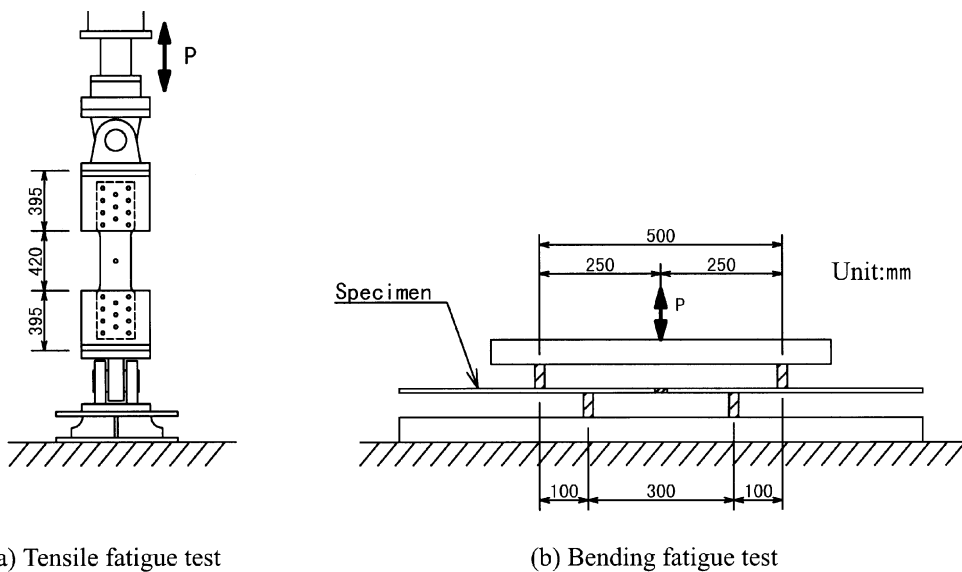


Fig. 3 Overall view of fatigue tests

Table 2 Results of fatigue tests

(a) Tensile fatigue test

Specimen	R	$\Delta\sigma_{mn}$ (MPa)	$\Delta\sigma_m$ (MPa)	$\frac{\Delta\sigma_m}{\sqrt{\sigma_Y}}$	N_i ($\times 10^4$ cycles)
T40-1	0.1	187.9	588.3	35.6	4.7
T40-2	0.1	187.9	588.3	35.6	4.9
T40-3	0.1	150.3	470.6	28.4	24.3
T40-4	0.1	169.1	529.5	32.0	7.5
T40-5	0.1	131.6	412.0	24.9	68.1
T40-6	0.1	112.8	353.2	21.3	259.6*
T40-7	0.1	126.9	397.3	24.0	93.0
T40-8	0.1	122.2	382.6	23.1	92.6
T40-9	0.1	117.5	367.9	22.2	380.0*
T40-10	0.1	122.2	382.6	23.1	294.9*
T40-11	0.1	112.5	352.4	21.3	1020.7*
T40-12	0.1	159.7	500.0	30.2	26.4
T40-13	0.1	190.2	595.5	36.0	9.9
T40-14	0.1	187.7	587.7	35.5	7.6
T40-15	0.5	105.6	330.9	20.0	550.3*
T49-1	0.1	136.9	441.0	22.0	537.4*
T49-2	0.1	189.1	609.1	30.4	39.1
T49-3	0.1	227.5	732.8	36.5	10.9
T49-4	0.5	134.6	433.5	21.6	310.6
T49-5	0.5	126.4	407.1	20.3	1091.7*

*: No cracks

(b) Bending fatigue test

Specimen	R	$\Delta\sigma_{bn}$ (MPa)	$\Delta\sigma_b$ (MPa)	$\frac{\Delta\sigma_b}{\sqrt{\sigma_Y}}$	N_i ($\times 10^4$ cycles)	
					One crack	The other crack
B40-1	0.1	207.4	372.3	22.5	320.0*	320.0*
B40-2	0.1	241.9	434.2	26.2	64.0	130.0
B40-3	0.1	293.8	527.4	31.8	26.0	-
B40-4	0.1	276.5	496.3	29.9	45.0	71.0
B40-5	0.1	224.6	403.2	24.3	141.6	184.0

*: No cracks

is the stress ratio, a ratio of lowest to highest stress in fatigue loading, $\Delta\sigma_{mn}$ is the range of nominal membrane stress on the gross cross section of Specimens T40 or T49, $\Delta\sigma_m$ is the stress range at the middle of the plate thickness of the hole in Specimens T40 or T49, as shown in Fig. 4, $\Delta\sigma_{bn}$ is the range of nominal plate-bending stress on the gross cross section of Specimens B40, $\Delta\sigma_b$ is the stress range on the chamfer of the hole edge in Specimens B40, as shown in Fig. 4, σ_Y is the measured yield stress, and N_i is the crack initiation life.

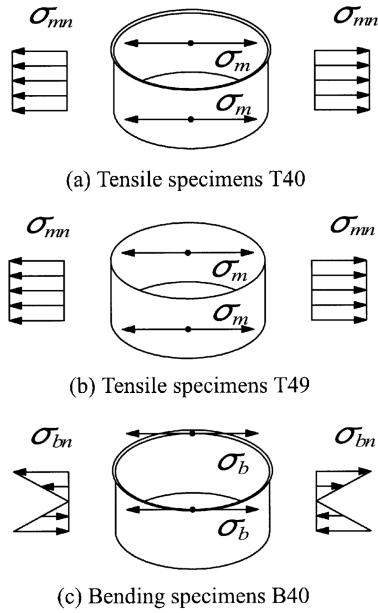


Fig. 4 Stresses $\Delta\sigma_m$ and $\Delta\sigma_b$

The relations between $\Delta\sigma_m$ and $\Delta\sigma_{mn}$ and between $\Delta\sigma_b$ and $\Delta\sigma_{bn}$ are as follows:

$$\text{For specimens T40, } \Delta\sigma_m = 3.131\Delta\sigma_{mn} \quad (2)$$

$$\text{For specimens T49, } \Delta\sigma_m = 3.221\Delta\sigma_{mn} \quad (3)$$

$$\text{For specimens B40, } \Delta\sigma_b = 1.795\Delta\sigma_{bn} \quad (4)$$

The FE analysis with solid elements, which will be described in Section 3.2., provides these relations.

The crack initiation life N_i is the number of cycles when the sudden change of strain given by the stress concentration gauges glued near the hole edge allows detection of a fine crack. The positions of the stress concentration gauges are provided in Fig. 5.

As shown in Fig. 6, two fatigue cracks were initiated on the surface of the plate thickness of the hole in Specimens T40 and T49, and on the chamfer of the hole edge in Specimens B40. In Specimens T40 and T49, the two cracks were observed at almost the same time. In Specimens B40, however, they were observed at pretty different cycles.

2.2. Fatigue limit of plates with a circular hole

Barsom and Rolfe (1987) proposed the following equation for the prevention of cracking at a notch tip of radius ρ :

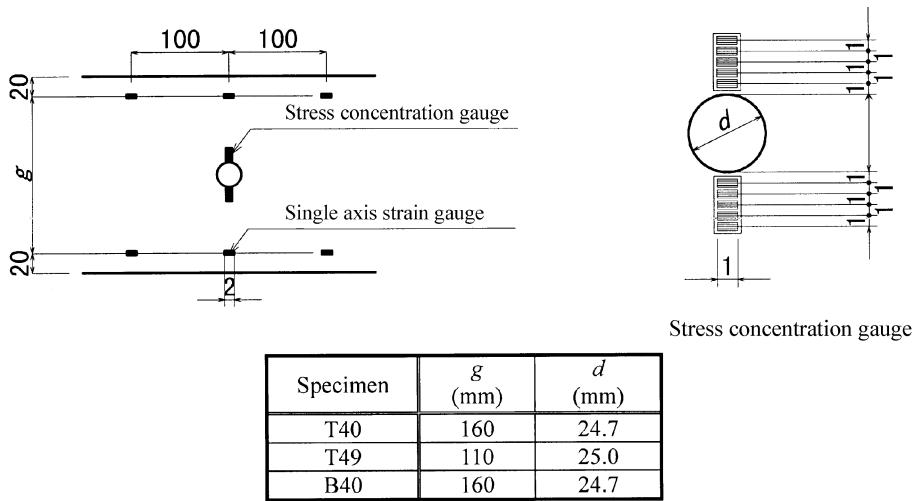


Fig. 5 Positions of stress concentration gauges

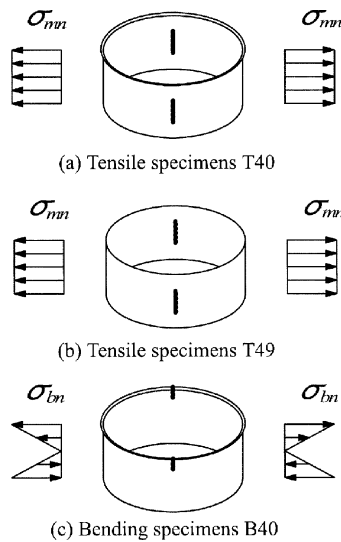


Fig. 6 Fatigue cracks observed

$$\frac{\Delta K}{\sqrt{\rho}} < 26.3 \sqrt{\sigma_Y} \tag{5}$$

where ΔK is the range of stress intensity factor for a crack of length equal to that of the notch ($\text{MPa}\sqrt{\text{m}}$), and ρ is the radius of the notch tip (m).

If we take $\Delta\sigma_{mn} \sqrt{\pi a} = \Delta K$, Eqs. (1) and (5) are the same except for the value of the coefficient.

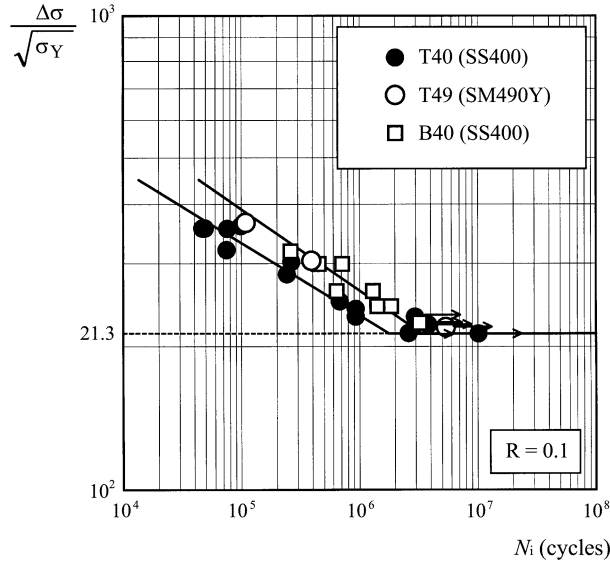


Fig. 7 Relation between $\Delta\sigma/\sqrt{\sigma_Y}$ and N_i [$R = 0.1$]

The relation between the stress range $\Delta\sigma$ at the notch tip and ΔK is approximated by (Okamura 1976):

$$\Delta\sigma \cong \frac{2\Delta K}{\sqrt{\pi\rho}} \quad (6)$$

Eliminating ΔK from Eqs. (5) and (6) gives

$$\frac{\Delta\sigma}{\sqrt{\sigma_Y}} < 29.7 \quad (7)$$

This equation means that the fatigue limit in terms of the stress range at a notch tip is normalized by the square root of the yield stress of steel. We apply this feature to our test results.

Fig. 7 shows the relation between $\Delta\sigma/\sqrt{\sigma_Y}$ and N_i for $R = 0.1$ in Table 2. Here $\Delta\sigma$ is $\Delta\sigma_m$ or $\Delta\sigma_b$. The results of the bending specimens are located above those of the tensile specimens. However, in the long life region, both results are scattered about the same mean value. Therefore, the fatigue limits of a circular hole under membrane stress and under plate-bending stress are the same. Since fatigue cracks are not produced below 21.3 of $\Delta\sigma/\sqrt{\sigma_Y}$, we take the following as the fatigue limit of plates with a circular hole:

$$\Delta\sigma = 21.3\sqrt{\sigma_Y} \quad (R = 0.1) \quad (8)$$

As shown in Table 2(a), Specimen T49-4 with $R = 0.5$ and $\Delta\sigma_m/\sqrt{\sigma_Y} = 21.6$ has fatigue cracks at 3.106×10^6 cycles, but Specimens T40-15 with $R = 0.5$ and $\Delta\sigma_m/\sqrt{\sigma_Y} = 20.0$ and Specimen T49-5 with $R = 0.5$ and $\Delta\sigma_m/\sqrt{\sigma_Y} = 20.3$ have no fatigue cracks at 5.503×10^6 cycles and 1.0917×10^7 cycles, respectively. Accordingly we take the value of Specimen T40-15 as the fatigue limit for $R = 0.5$.

Thus

$$\Delta\sigma = 20.0\sqrt{\sigma_Y} \quad (R = 0.5) \tag{9}$$

For both of membrane and plate-bending stresses, the conditions to prevent a circular hole from the re-initiation of fatigue cracks are as follows:

$$\Delta\sigma_t < \begin{cases} 21.3\sqrt{\sigma_Y} & (R = 0.1) \\ 20.0\sqrt{\sigma_Y} & (R = 0.5) \end{cases} \tag{10}$$

where $\Delta\sigma_t$ is the stress range on the circumference of a circular hole.

3. Equations to estimate maximum stress at stop-holes

Since stop-holes are placed at crack tips, the stress range on the circumference of a circular hole with a crack has to be used for $\Delta\sigma_t$ in Eq. (10). First we provide the equations to estimate σ_t for the case where normal and shearing stresses act simultaneously, and later for the case in which membrane and plate-bending stresses act simultaneously.

3.1. Maximum stress at stop-holes under normal and shearing stresses

Let us consider the following case: As shown in Fig. 8(a), when a fatigue crack propagates vertically on a plate, and its length becomes $2a$, we put stop-holes with a radius of ρ at both ends of the crack. Here membrane stress σ_{mn} (normal stress) and τ_{mn} (shearing stress) are each assumed to be distributed uniformly. Now, as shown in Fig. 8(b), we consider the case of $a = \rho$, namely, the case in which only a

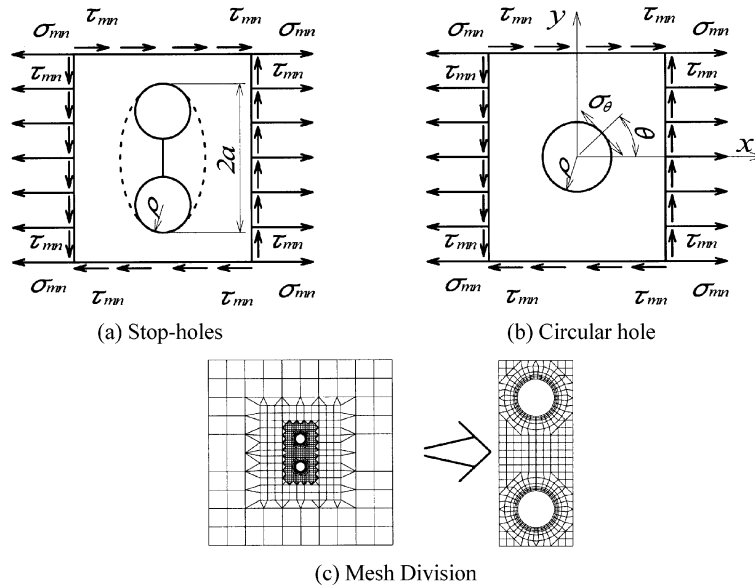


Fig. 8 Stop-hole under normal and shearing stresses

circular hole exists. Where σ_{mn} and τ_{mn} act infinitely far away, the stress σ_θ in the tangential direction of the circumference of the hole is given by (Timoshenko and Goodier 1951)

$$\sigma_\theta = \sigma_{mn}(1-2\cos 2\theta) - 4\tau_{mn}\sin 2\theta \quad (11)$$

The maximum value σ_m of σ_θ and its direction θ_m are given, respectively, by

$$\sigma_m = \sigma_{mn} + 2\sqrt{\sigma_{mn}^2 + 4\tau_{mn}^2} \quad (12)$$

$$\theta_m = -\frac{\pi}{2} + \frac{1}{2}\tan^{-1}\frac{2\tau_{mn}}{\sigma_{mn}} \quad (13)$$

When $\tau_{mn} = 0$ in Fig. 8(a), that is, only normal stress σ_{mn} acts, the elliptic approximation gives the following equation for the maximum stress σ_t on stop-holes (Japan Society of Materials Science 1995):

$$\sigma_t = \left(1 + 2\sqrt{\frac{a}{\rho}}\right)\sigma_{mn} \quad (14)$$

Assuming that this elliptic approximation is also applicable for the case in which τ_{mn} and σ_{mn} act simultaneously, the maximum stress σ_t at stop-holes is given by

$$\sigma_t = \frac{1}{3}\left(1 + 2\sqrt{\frac{a}{\rho}}\right)(\sigma_{mn} + 2\sqrt{\sigma_{mn}^2 + 4\tau_{mn}^2}) \quad (15)$$

Fig. 9 shows the comparison of this equation with the results from FE analysis. Fig. 8(c) shows the model used for the FE analysis. The finite elements used are 8-node thick shell elements (Element type 22 in MARC 1994). Eq. (15) approximates the FE results very well.

In order to consider the effects of the chamfer at the hole edge and also the feature that the stress on

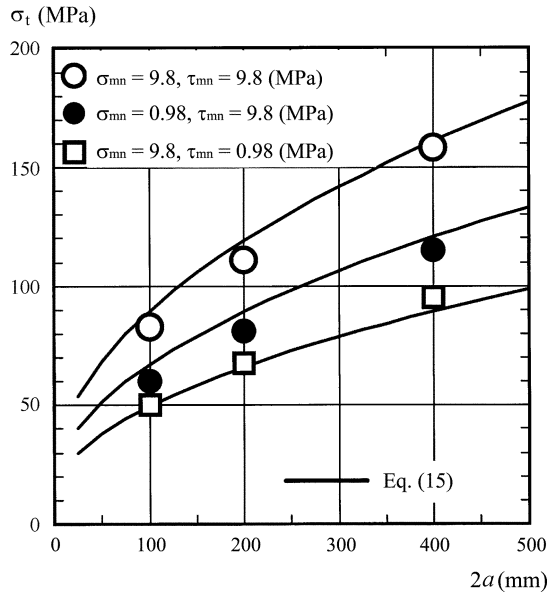


Fig. 9 Comparison of Eq. (15) with FE results

the middle of plate thickness of a circular hole is somewhat higher than that on the hole edge, we have to multiply Eq. (15) by 1.07, and obtain

$$\sigma_t = \frac{1.07}{3} \left(1 + 2 \sqrt{\frac{a}{\rho}} \right) (\sigma_{mn} + 2 \sqrt{\sigma_{mn}^2 + 4 \tau_{mn}^2}) \quad (16)$$

The grounds for the value 1.07 will be given in the next section.

3.2. Maximum stress at stop-holes under membrane and plate-bending stresses

In actual bridges, membrane stresses can be distributed, and also plate-bending stresses can be created. In such cases, usually we have to use FE analysis with shell elements to obtain the stresses on the circumference of the stop-holes. Next we establish an equation to be used in estimating the maximum stress at the stop-holes by the results from FE analysis with shell elements.

First we investigate the stresses at a circular hole under membrane stress or plate-bending stress by FE analysis with solid elements. Fig. 10 shows the FE model. The finite elements used are 20-node isoparametric solid elements (Element type 21 in MARC 1994). Table 3 lists the stress concentration factors obtained from this analysis. Table 3(a) is for the case of no chamfer, and Table 3(b) is for the case of the chamfer of $s = 1.0 \text{ mm}$ and $\theta = 45^\circ$. The definition of the stress concentration factors is as follows:

$$K_m = \frac{\sigma_m}{\sigma_{mn}} \quad (17)$$

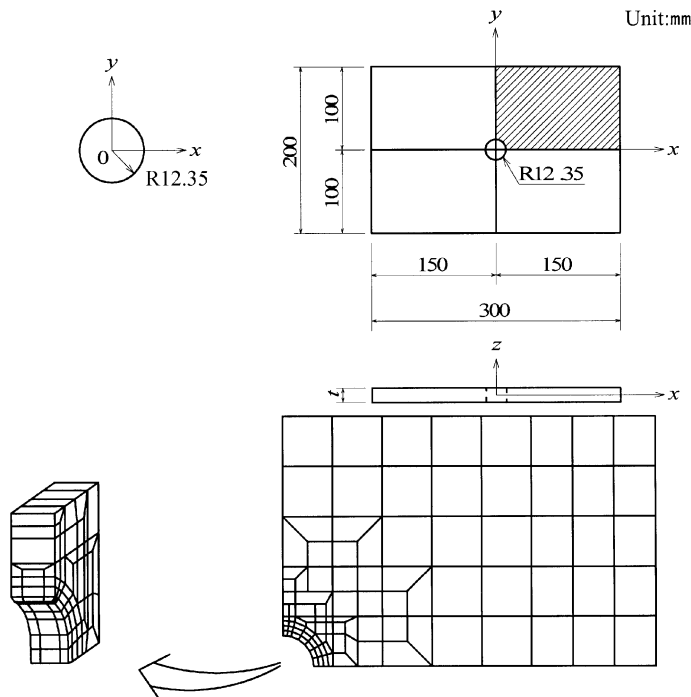


Fig. 10 FE model with solid elements

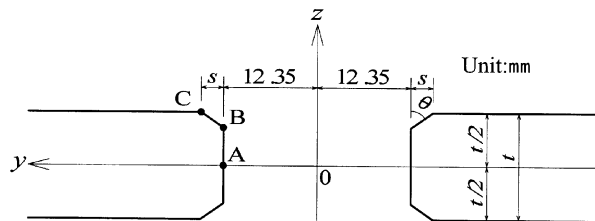
Table 3 Stress concentration factors

(a) $s = 0.0$ mm

t (mm)	8.75	17.50	26.25	35.00
K_m (A)	3.116	3.172	3.189	3.184
K_m (B)	2.965	2.834	2.754	2.722
K_b (A)	0.000	0.000	0.000	0.000
K_b (B)	1.918	2.018	2.105	2.185
K_{bR}	1.985	2.152	2.278	2.376

(b) $s = 1.0$ mm, $\theta = 45^\circ$

t (mm)	8.75	17.50	26.25	35.00
K_m (A)	3.172	3.191	3.198	3.191
K_m (B)	3.115	3.010	2.937	2.896
K_m (C)	2.561	2.422	2.334	2.295
K_b (A)	0.000	0.000	0.000	0.000
K_b (B)	1.593	1.907	2.065	2.177
K_b (C)	1.772	1.807	1.856	1.906



$$K_b = \frac{\sigma_b}{\sigma_{bn}} \tag{18}$$

where K_m and K_b are the stress concentration factors for membrane and plate-bending stresses, respectively. A, B and C in the parenthesis after K_m and K_b represent the points A, B and C in the inserted figure in the table, respectively.

As seen from Table 3, $K_m(A)$ is somewhat greater than $K_m(B)$. Peterson (1953) already pointed out that the stress concentration factor at the middle of the plate thickness is somewhat greater than that at the hole edge. However, the variation of $K_m(A)$ is very small with respect to the plate thickness. Thus, we take 3.2 for K_m as a value that is applicable on the safe side for both cases with and without the chamfer.

Table 3 also indicates that K_b increases with the increase in plate thickness. This is due to the effects of the transverse shear deformation on the bending of plates. Reissner (1945) provided the following stress concentration factor for an infinite plate with a circular hole under plate-bending, considering the

effects of transverse shear deformation:

$$K_{bR} = \frac{3}{2} + \frac{3(1+\nu)K_2\left(\frac{\sqrt{10}\rho}{t}\right) - 2K_0\left(\frac{\sqrt{10}\rho}{t}\right)}{2(1+\nu)K_2\left(\frac{\sqrt{10}\rho}{t}\right) + 4K_0\left(\frac{\sqrt{10}\rho}{t}\right)} \quad (19)$$

where $K_n(\cdot)$ is the modified Bessel function of the second kind, of order n (Duffy 1998), and ν is the Poisson's ratio.

Reissner's stress concentration factor has the following features:

$$\lim_{\rho/t \rightarrow 0} K_{bR} = 3 \quad (20)$$

$$\lim_{\rho/t \rightarrow \infty} K_{bR} = \frac{5+3\nu}{3+\nu} \quad (21)$$

Eq. (21) is the same as the stress concentration factor obtained from the classical thin-plate theory, which does not consider the effects of the transverse shear deformation on the bending of plates (Nakayama 1927). Eq. (21) gives the value 1.788 for $\nu = 0.3$.

For $\nu = 0.3$, Eq. (19) can be approximated by

$$K_{bR} = \frac{3.157 + \frac{6.193\rho}{t}}{1 + \frac{3.539\rho}{t}} \quad (22)$$

For $0.05 \leq \rho/t \leq 4$, Eq. (22) approximates Eq. (19) with a relative error less than 1%.

The values of K_{bR} from Eq. (22) are given in Table 3(a). K_{bR} is larger than $K_b(B)$ for the case of no chamfer, and also larger than $K_b(B)$ and $K_b(C)$ for the case of chamfer. Thus we take Eq. (22) on the safe side as the stress concentration factor at a circular hole under plate-bending stress.

Adding the maximum stress for membrane stress to that for plate-bending stress, the maximum stress at a circular hole under membrane and plate-bending stresses is given by

$$\sigma_t = \sigma_m + \sigma_b = K_m \sigma_{mn} + K_b \sigma_{bn} \quad (23)$$

Using 3.2 for K_m and Eq. (22) for K_b , we obtain

$$\sigma_t = 3.2\sigma_{mn} + \frac{3.157 + \frac{6.193\rho}{t}}{1 + \frac{3.539\rho}{t}} \sigma_{bn} \quad (24)$$

When we use shell elements in FE analysis, we have to consider the following: The influence of the chamfer at the hole edge can not be taken into account in shell elements. Even if we use very fine shell elements, the stress concentration factor is 3.0 for a circular hole under membrane stress. Similarly, where we use shell elements based on classical thin-plate theory, the stress concentration factor is 1.788 for plate-bending stress.

Thus, when we use the results from FE analysis with shell elements, we have to estimate the maximum stress at stop-holes by the following equation:

$$\sigma_t = 1.07 \sigma_{m(FEM)} + \eta \sigma_{b(FEM)} \quad (25)$$

where $\sigma_{m(FEM)}$ and $\sigma_{b(FEM)}$ are, respectively, the membrane and plate-bending stresses in the tangential direction on the circumference of the stop-holes computed by FE analysis with shell elements, and η is as follows:

$$\eta = \frac{1.766 + \frac{3.464\rho}{t}}{1 + \frac{3.539\rho}{t}} \quad (26)$$

Dividing the coefficient 3.2 in Eq. (24) by 3.0 gives the coefficient 1.07 in Eq. (25), and likewise dividing $(3.157+6.193 \rho / t)/(1+3.539 \rho / t)$ in Eq. (24) by 1.788 gives η in Eq. (25).

Where we use shell elements considering the effects of the transverse shear deformation on the bending of plates, we have to take one for η . In Eq. (25) the effects of a chamfer less than 1 mm at the hole edge are considered. The value 1.07 in Eq. (25) was also introduced into Eq. (16).

The stress ranges given by Eq. (16) for the case in which normal and shearing stresses act simultaneously, and by Eq. (25) for the case where membrane and plate-bending stresses act simultaneously, must satisfy Eq. (10) to prevent the re-initiation of fatigue cracks at stop-holes.

4. Conclusions

The conditions under which stop-holes prevent the re-initiation of fatigue cracks were given by Eq. (10). As the equations necessary to estimate the maximum stress on the circumference of the stop-holes, Eq. (16) was provided for the case in which normal and shearing stresses act simultaneously, and Eq. (25) for the case where membrane and plate-bending stresses act simultaneously. If the stress range given by Eq. (16) or Eq. (25) satisfies Eq. (10), fatigue cracks would not be expected to occur from stop-holes.

References

- Barsom, J.M. and Rolfe, S.T. (1987), *Fracture & Fatigue Control in Structures*, Second Edition, Prentice-Hall, Inc., USA, 266-268.
- Duffy, D.G. (1998), *Advanced Engineering Mathematics*, CRC Press LLC, USA, 305-323.
- Fisher, J.W. (1984), *Fatigue and Fracture in Steel Bridges*, John Wiley & Sons, New York, USA.
- Fisher, J.W., Barthelemy, B.M., Mertz, D.R. and Edinger, J.A. (1980) "Fatigue behavior of full-scale welded bridge attachments", NCHRP Report 227, Transportation Research Board, National Research Council, USA, November.
- Fisher, J.W., Jin, J., Wagner, D.C. and Yen, B.T. (1990), "Distortion-induced fatigue cracking in steel bridges", NCHRP Report 336, Transportation Research Board, National Research Council, USA, December.
- Japan Road Association (1997), *Fatigue in Steel Bridges*, Maruzen, Co., Ltd., Japan, 58-62 and 285-289. (in Japanese)
- Japan Society of Materials Science (1995), *A Handbook for Fatigue Design*, Yokendo, Co., Ltd., Japan, 19-23.

(in Japanese)

Japanese Industrial Standard (1994), "Abrasive papers", R6252. (in Japanese)

MARC (1994), Marc Analysis Research Corporation, Version K6.2, USA.

Nakayama, I. (1927), "The effect of an elliptic hole in a plate subjected to bending", JSME, Japan, **30**(119), 109-126.

Okamura, H. (1976), Introduction to Linear Fracture Mechanics, Baihukan, Co., Ltd., Japan, 26-29. (in Japanese)

Okura, I. and Ishikawa, T. (1999), "Conditions to keep drilled holes from fatigue cracking", JSSC, Japan, *J. Constructional Steel*, **7**, 181-188. (in Japanese)

Okura, I., Shiozaki, T. and Nakanishi, Y. (1996), "Fatigue strength of drilled holes under membrane and plate-bending stresses", JSCE, Japan, *Structural Eng./Earthquake Eng.*, 537/I-35, 327-338. (in Japanese)

Peterson, R.E. (1953), *Stress Concentration Design Factors*, John Wiley & Sons, Inc., USA, 78.

Reissner, E. (1945), "The effect of transverse shear deformation on the bending of elastic plates", *J. Applied Mechanics*, USA, A69-A77, June.

Timoshenko, S. and Goodier, J.N. (1951), *Theory of Elasticity*, Second Edition, McGraw-Hill Book Company, Inc., USA, 78-85.

CC